# Delamination of Multilayered Non-linear Elastic Shafts in Torsion

**Victor Rizov**
Professor
University of Architecture, Civil Engineering and Geodesy
Departmemt of Technical Mechanics
Sofia
Bulgaria

*Delamination cracks in multilayered circular shafts loaded in torsion are analyzed in terms of the strain energy release rate. It is assumed that the material in each layer has non-linear mechanical behaviour that is treated by the Ramberg-Osgood constitutive law. Also, each layer exhibits smooth material inhomogeneity in radial direction. It is assumed that the three material properties involved in the Ramberg-Osgood constitutive law vary continuously in radial direction of layers. A methodology for determination of the strain energy release rate is developed that is applicable for shafts made of arbitrary number of adhesively bonded concentric layers which have individual thickness and material properties. The delamination cracks are located arbitrary between layers. The methodology is used to investigate a delamination in a multilayered clamped shaft. The delamination is also studied by analyzing the energy balance for verification. Parametric analyses of the clamped multilayered shaft are carried-out.*

***Keywords:*** *Multilayered circular shaft, Delamination fracture, Material inhomogeneity, Torsion, Material non-linearity*

## 1. INTRODUCTION

The delamination fracture behaviour of layered materials and structures has been the subject of investigation by many researchers from both theoretical and applied standpoints in the last few decades. This is due to the fact that the delamination, i.e. separation of layers, is one of the most important causes for disintegration of layered structural members. The delamination phenomenon is studied usually in terms of the strain energy release rate by assuming linear-elastic behaviour of the material [1].

Recently, several papers on delamination fracture in multilayered beam configurations which exhibit non-linear mechanical behaviour of the material have been published [2-4]. These publications are focused on delamination in multilayered beams of a rectangular cross-section. The beams are loaded in bending. Various solutions to the strain energy release rate are derived for the cases when the layers of beams are made of inhomogeneous or functionally graded materials. It is assumed that layers exhibit continuous (smooth) inhomogeneity (usually, the modulus of elasticity varies continuously in the cross-section of layers). It should be noted that the strong interest towards the inhomogeneous materials is due mainly to the fact that the functionally graded materials as a new kind of inhomogeneous composites which consist of two or more constituents with gradual variation of their microstructure over volume are ubiquitous in aeronautics, nuclear reactors, microelectronics, biomedicine and optics [5-9]. Although the ordinary laminated composites are widely used in engineering [10-16], the sharp interfaces between their constituents lead often to failure from interfacial stress concentrations. Actually, one of the important advantages of functionally graded materials in comparison with the laminated composites is the elimination of interfacial stress concentrations.

It should be mentioned that fracture analyses of continuously inhomogeneous (functionally graded) materials and structures are carried-out by using methods of linear-elastic fracture mechanics which are applicable for linear-elastic behaviour only [17]. Obviously, it would be useful to develop fracture analyses with taking into account the non-linear elastic behaviour of the material. In the present paper, the delamination fracture behaviour of multilayered non-linear elastic circular shafts loaded in torsion is investigated assuming that layers exhibit continuous inhomogeneity in radial direction. The main objective is to develop a methodology for determination of the strain energy release rate when the non-linear elastic behaviour of the material is described by the Rambeg-Osgood constitutive equation assuming that the three material properties involved in the constitutive equation vary gradually in radial direction in contrast to previous studies which deal with the case when only one material property (usually, the shear modulus) vary in radial direction [18].

## 2. METHODOLOGY FOR ANALYSIS OF THE STRAIN ENERGY RELEASE RATE

Delamination cracks in multilayered non-linear elastic circular shafts loaded in torsion are under consideration in the present paper. Shafts are made of concentric longitudinal adhesively bonded layers. The number of layers is denoted by $n$. Each layer exhibits smooth material inhomogeneity in radial direction. The non-linear mechanical behaviour of the material in each layer is treated by the Ramberg-Osgood constitutive law. Delamination cracks are located arbitrary between layers. A portion of a multilayered shaft with delamination crack front is depicted in Figure 1. The delamination crack front is a

Received: August 2019, Accepted: May 2020
Correspondence to: Professor Victor Rizov
University of Architecture, Civil Engineering and Geodesy, 1046 – Sofia, Bulgaria
E-mail: v_rizov_fhe@uacg.bg
**doi: 10.5937/fme2003681R**

circle of radius, $r_1$. The internal crack arm is a circular shaft with radius, $r_1$.

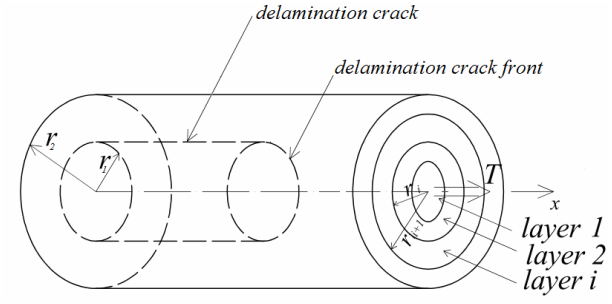


**Figure 1. Portion of a circular multilayered shaft with the delamination crack front (the delamination crack is a cylindrical surface with radius, $r_1$)**

The external crack arm is a ring-shaped shaft with internal radius, $r_1$, and external radius, $r_2$. The torsion moment in the shaft cross-section ahead of the delamination crack front is denoted by $T$. The delamination fracture behaviour is analyzed in terms of the strain energy release rate by using the following formula [19]:

$$G=\frac{1}{r_1}\left(\sum_{i=1}^{i=n_1}\int_{r_i}^{r_{i+1}} u^*_{0a_1 i}\,r\,dr+ \right. \\ \left. +\sum_{i=1}^{i=n_2}\int_{r_i}^{r_{i+1}} u^*_{0a_2 i}\,r\,dr-\sum_{i=1}^{i=n}\int_{r_i}^{r_{i+1}} u^*_{0i}\,r\,dr\right) \tag{1}$$

where $n_1$ and $n_2$ are the numbers of layers, respectively, in the internal and external crack arms, $r_i$ and $r_{i+1}$ are, respectively, the radiuses of the internal and external surfaces of the $i$-th layer, $u^*_{0a_1 i}$, $u^*_{0a_2 i}$ and $u^*_{0i}$ are the complementary strain energy densities in $i$-th layer of the internal and external crack arms in the cross-section behind the crack front and in $i$-th layer in the shaft cross-section ahead of the crack front, respectively.

The relation between the shear strain, $\gamma$, and the shear stress, $\tau_i$, in the $i$-th layer of the internal crack arm is expressed by the Ramberg-Osgood constitutive law

$$\gamma=\frac{\tau_i}{Q_i}+\left(\frac{\tau_i}{H_i}\right)^{\frac{1}{m_i}} \tag{2}$$

where $Q_i$, $H_i$ and $m_i$ are material properties which vary continuously in radial direction in each layer

$$Q_i=Q_i(r) \tag{3}$$

$$H_i=H_i(r) \tag{4}$$

$$m_i=m_i(r) \tag{5}$$

The complementary strain energy density in $i$-th layer of the internal crack arm is calculated by the following formula [20]:

$$u^*_{0a_1 i}=\frac{\tau_i^2}{2Q_i}+\frac{m_i\tau_i^{\frac{1+m_i}{m_i}}}{(1+m_i)H_i^{\frac{1}{m_i}}} \tag{6}$$

One of the characteristic features of the Ramberg-Osgood constitutive law (2) is that the stress, $\tau_i$, can not be determined explicitly. Therefore, $\tau_i$ is expanded in series of Taylor by keeping the first three members

$$\tau_i(r)\approx\tau_i(r_{bi})+\frac{\tau_i'(r_{bi})}{1!}(r-r_{bi})+ \\ +\frac{\tau_i''(r_{bi})}{2!}(r-r_{bi})^2 \tag{7}$$

where

$$r_{bi}=\frac{r_i+r_{i+1}}{2} \tag{8}$$

$$i=1,2,3,\ldots n_1 \tag{9}$$

By introducing of coefficients, $q_{\alpha i}$, $q_{\beta i}$ and $q_{\delta i}$, formula (7) is re-written as

$$\tau_i(r)\approx q_{\alpha i}+q_{\beta i}(r-r_{bi})+q_{\delta i}(r-r_{bi})^2 \tag{10}$$

In order to use the Ramberg-Osgood constitutive law (2) for determination of $q_{\alpha i}$, $q_{\beta i}$ and $q_{\delta i}$, the shear strain has to presented as a function of the radius, $r$. By applying the Bernoulli's hypothesis for plane sections, the distribution of the shear strains in the internal crack arm is written as

$$\gamma=\frac{r}{r_1}\gamma_b \tag{11}$$

where

$$0\le r\le r_1 \tag{12}$$

In (11), $\gamma_b$ is the shear strain at the periphery of the internal crack arm. It should be mentioned that the applicability of the Bernoulli's hypothesis for plane sections follows from the fact that circular shafts of high length to diameter ratio are under consideration in the present paper.

By combining of (2), (10) and (11), one arrives at

$$\frac{r}{r_1}\gamma_b=\frac{q_{\alpha i}+q_{\beta i}(r-r_{bi})+q_{\delta i}(r-r_{bi})^2}{Q_i}+ \\ +\frac{\left[q_{\alpha i}+q_{\beta i}(r-r_{bi})+q_{\delta i}(r-r_{bi})^2\right]^{\frac{1}{m_i}}}{H_i^{\frac{1}{m_i}}} \tag{13}$$

In order to obtain equations for determination of $q_{\alpha i}$, $q_{\beta i}$ and $q_{\delta i}$, first, $r=r_{bi}$ is substituted in (13). The result is

$$\frac{r_{bi}}{r_1}\gamma_b=\frac{q_{\alpha i}}{Q_i}+\frac{q_{\alpha i}^{\frac{1}{m_i}}}{H_i^{\frac{1}{m_i}}} \tag{14}$$

Further, by substituting of $r=r_{bi}$ in the first and second derivatives of (13) with respect to $r$, one arrives at

$$\frac{\gamma_b}{r_1}=\frac{q_{\beta i}Q_i-q_{\alpha i}Q_i^{'}}{Q_i^2}+$$
$$\frac{q_{\alpha i}^{\psi_i}}{H_i^{\psi_i}}\left[\ \psi_i^{'}\left(\ln q_{\alpha i}-\ln H_i\right)+\psi_i\left(\frac{q_{\beta i}}{q_{\alpha i}}-\frac{H_i^{'}}{H_i}\right)\ \right] \tag{15}$$
$$0=\frac{\left(2q_{\delta i}Q_i-q_{\alpha i}Q_i^{''}\right)Q_i^2}{Q_i^4}-\frac{\left(qa_{\beta i}Q_i-q_{\alpha i}Q_i^{'}\right)2Q_iQ_i^{'}}{Q_i^4}+$$
$$+\frac{q_{\alpha i}^{\psi_i}}{H_i^{\psi_i}}\left[\psi_i^{'}\left(\ln q_{\alpha i}-\ln H_i\right)+\psi_i\left(\frac{q_{\beta i}}{q_{\alpha i}}-\frac{H_i^{'}}{H_i}\right)\right]^2+$$
$$\frac{q_{\alpha i}^{\psi_i}}{H_i^{\psi_i}}\left\{\psi_i^{''}\left(\ln q_{\alpha i}-\ln H_i\right)+2\psi_i^{'}\left(\frac{q_{\beta i}}{q_{\alpha i}}-\frac{H_i^{'}}{H_i}\right)+\right. \tag{16}$$
$$\left.\psi_i\left[-\frac{q_{\beta i}^2}{q_{\alpha i}^2}+\frac{2q_{\delta i}}{q_{\alpha i}}+\frac{\left(H_i^{'}\right)^2}{H_i^2}-\frac{H_i^{''}}{H_i}\right]\right\}$$

where $Q_i$, $H_i$ and $m_i$, and their derivatives, $Q^{`}_i$, $Q^{``}_i$, $H^{`}_i$, $H^{``}_i$, $m^{`}_i$ and $m^{``}_i$, are calculated at $r = r_{bi}$. In equations (14), (15) and (16),

$$i=1,\,2,\,3,\ldots n_1 \tag{17}$$

$$\psi_i=\frac{1}{m_i} \tag{18}$$

Equations (14), (15) and (16) are worked out for each layer in the internal crack arm. Thus, $3n_1$ equations whit $3n_1$+1 unknowns, $\gamma_b$, $q_{\alpha i}$, $q_{\beta i}$ and $q_{\delta i}$, where = 1,2,3,...,$n_1$ are worked out. Another equation is worked out by considering the equilibrium of the elementary forces in the internal crack arm cross-section

$$T_1=\sum_{i=1}^{i=n_1}\ 2\pi\int_{r_i}^{r_{i+1}}\tau_i\,r^2\,dr \tag{19}$$

where $T_1$ is the torsion moment in the internal crack arm cross-section behind the delamination crack front. By substituting of (10) in (19), one derives

$$T_1=2\pi\sum_{i=1}^{i=n_1}\left[\frac{q_{\alpha i}}{3}\left(r_{i+1}^3-r_i^3\right)+\frac{q_{\beta i}}{4}\left(r_{i+1}^4-r_i^4\right)-\right.$$
$$\frac{q_{\beta i}}{3}r_{bi}\left(r_{i+1}^3-r_i^3\right)+\frac{q_{\delta i}}{5}\left(r_{i+1}^5-r_i^5\right)- \tag{20}$$
$$\left.-\frac{q_{\delta i}}{2}r_{bi}\left(r_{i+1}^4-r_i^4\right)+\frac{q_{\delta i}}{3}r_{bi}^2\left(r_{i+1}^3-r_i^3\right)\right]$$

Equations (14), (15), (16) and (20) should be solved with respect to $\gamma_b$, $q_{\alpha i}$, $q_{\beta i}$ and $q_{\delta i}$,, where $i$ = 1,2,3, ... $n_1$, , by using the MatLab computer program for particular shaft geometry, external loading and material properties. Then, the complementary strain energy density in each layer of the internal crack arm is calculated by substituting of (10) in (6).

The complementary strain energy density in the $i$-th layer of the external crack arm is written as

$$u_{0a2i}^{*}=\frac{\tau_{di}^2}{2Q_i}+\frac{m_i\tau_{di}^{\frac{1+m_i}{m_i}}}{\left(1+m_i\right)H_i^{\frac{1}{m_i}}} \tag{21}$$

where the shear stress, $\tau_{di}$, is expanded in series of Taylor

$$\tau_{di}(r)\approx p_{\alpha i}+p_{\beta i}\left(r-r_{bi}\right)+p_{\delta i}\left(r-r_{bi}\right)^2 \tag{22}$$

The coefficients, $p_{\alpha i}$, $p_{\beta i}$ and $p_{\delta i}$, where $i$ = 1,2,3, ..$n_2$, are determined by using equations (14), (15), (16) and (20). For this purpose, $T_1$, $n_1$, $\gamma_b$, $q_{\alpha i}$, $q_{\beta i}$ and $q_{\delta i}$ are replaced with $T_2$, $n_2$, $\gamma_d$, $p_{\alpha i}$, $p_{\beta i}$ and $p_{\delta i}$, respectively. Here, $T_2$ is the torsion moment in the external crack arm behind the delamination crack front, $\gamma_d$ is the shear strain at the periphery of the external crack arm.

The shear stress, $\tau_{fi}$, in the $i$-th layer of the shaft cross-section ahead of the delamination crack front is also expanded in series of Taylor

$$\tau_{fi}(r)\approx s_{\alpha i}+s_{\beta i}\left(r-r_{bi}\right)+s_{\delta i}\left(r-r_{bi}\right)^2 \tag{23}$$

Equations (14), (15), (16) and (20) are used to determine the unknown coefficients, $s_{\alpha i}$, $s_{\beta i}$ and $s_{\delta i}$, where $i$ = 1,2,3,...$n$. For this purpose, $T_1$, $n_1$, $\gamma_b$, $q_{\alpha i}$, $q_{\beta i}$ and $q_{\delta i}$ are replaced, respectively, with $T$, $n$, $\gamma_f$ , $s_{\alpha i}$, $s_{\beta i}$ and $s_{\delta i}$, where $T$ is the torsion moment in the shaft cross-section ahead of the delamination crack front, $\gamma_f$ is the shear strain at the periphery of the shaft. The complementary strain energy density in the $i$-th layer of the shaft cross-section ahead of the delamination crack front is expressed as

$$u_{0i}^{*}=\frac{\tau_{fi}^2}{2Q_i}+\frac{m_i\tau_{fi}^{\frac{1+m_i}{m_i}}}{\left(1+m_i\right)H_i^{\frac{1}{m_i}}} \tag{24}$$

where $\tau_{fi}$ is found by (23).

The strain energy release rate for the delamination crack in the multilayered circular shaft shown in Fig. 1 is obtained by substituting of (6), (21) and (24) in (1). The integration should be carried-out by using the MatLab computer program for particular shaft structure.

## 3. APPLICATION OF THE METHODOLOGY

The methodology for analyzing the strain energy release rate developed in section 2 of the present paper is applied here to investigate delamination fracture behaviour of a clamped multilayered circular shaft loaded in torsion. The shaft is shown schematically in Figure 2. A delamination cylindrical crack of length, $a$ , is located arbitrary between the concentric layers.

The radius of the internal crack arm cross-section is $r_1$. The length of the shaft is $l$. The shaft is clamped in its right-hand end. The loading on the shaft consists of one torsion moment, $T$, applied at the free end of the external crack arm as shown in Figure 2. Thus, the internal crack arm is free of stresses.

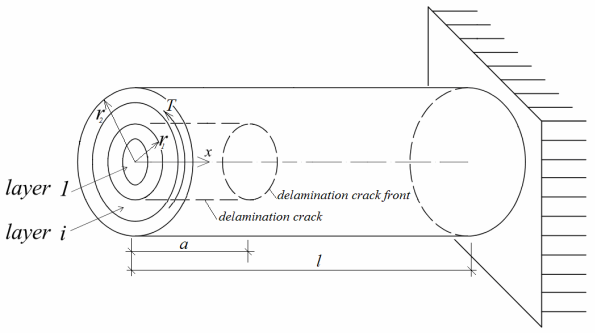


**Figure 2. Geometry and loading of a clamped multilayered circular shaft**

The continuous variation of the material properties, $Q_i$, $H_i$ and $m_i$, in radial direction of the $i$-th layer of the shaft is described by the following tangent laws:

$$Q_i = Q_{0i}\left[1 + g_{qi} tg\left(\frac{r - r_i}{r_{i+1} - r_i}\frac{\pi}{4}\right)\right] \tag{25}$$

$$H_i = H_{0i}\left[1 + g_{hi} tg\left(\frac{r - r_i}{r_{i+1} - r_i}\frac{\pi}{4}\right)\right] \tag{26}$$

$$m_i = m_{0i}\left[1 + g_{mi} tg\left(\frac{r - r_i}{r_{i+1} - r_i}\frac{\pi}{4}\right)\right] \tag{27}$$

where

$$r_i \le r \le r_{i+1} \tag{28}$$

In formulae (25) – (27), $Q_{0i}$, $H_{0i}$ and $m_{0i}$ are the values, respectively, of $Q_i$, $H_i$ and $m_i$ at the internal surface of layer $g_{qi}$, $g_{hi}$ and $g_{mi}$ are material properties which govern the material inhomogeneity in radial direction.

Since the internal crack arm is free of stresses,

$$u^*_{0a_1 i} = 0 \tag{29}$$

where

$$i = 1, 2, 3, ...n_1 \tag{30}$$

The complementary strain energy density in the $i$-th layer of the external crack arm is obtained by formula (21). For this purpose, $T_1$, $n_1$, $\gamma_b$, $q_{\alpha i}$, $q_{\beta i}$ and $q_{\delta i}$ are replaced, respectively, with $T_2$, $n_2$, $\gamma_d$, $p_{\alpha i}$, $p_{\beta i}$ and $p_{\delta i}$, in equations (14), (15), (16) and (20). After substituting of (25), (26) and (27) in (14), (15), (16), the equations are solved with respect to $\gamma_d$, $p_{\alpha i}$, $p_{\beta i}$ and $p_{\delta i}$, by using the MatLab computer program. Then, $u^*_{0a_2 i}$ is expressed by substituting of (22) in (12).

Formula (24) is applied in order to calculate the complementary strain energy density in the $i$-th layer in the shaft cross-section ahead of the delamination crack front. The quantities, $\gamma_f$ , $s_{\alpha i}$, $s_{\beta i}$ and $s_{\delta i}$, are determined from equations (14), (15), (16) and (20) by replacing of $T_1$, $n_1$, $\gamma_b$, $q_{\alpha i}$, $q_{\beta i}$ and $q_{\delta i}$ with $T$, $n$, $T$ , $n$ , $\gamma_f$ , $s_{\alpha i}$, $s_{\beta i}$ and $s_{\delta i}$, respectively.

Finally, the strain energy release rate for the cylindrical delamination crack in the clamped shaft shown Figure 2 is obtained by substituting of (21), (24) and (29) in (1). The integration in (1) is performed by the MatLab computer program.

The delamination fracture behaviour of the multilayered clamped shaft (Figure 2) is studied also by analyzing the energy balance in order to verify the solution to the strain energy release rate. For this purpose, a small increase of the delamination crack length, $\delta a$, is assumed leading to the following equation for balance of the energy:

$$T\delta\phi = \frac{\partial U}{\partial a}\delta a + G l_{dl}\delta a \tag{31}$$

where $\varphi$ is the angle of twist of the free end of the external crack arm, $U$ is the strain energy cumulated in the shaft, $l_{dl}$ is the length of the delamination crack front. From (31), one derives the following expression for the strain energy release rate:

$$G = \frac{T}{l_{dl}}\frac{\partial\phi}{\partial a} - \frac{1}{l_{dl}}\frac{\partial U}{\partial a} \tag{32}$$

The delamination crack front length is

$$l_{dl} = 2\pi r_1 \tag{33}$$

Therefore, formula (32) is re-written as

$$G = \frac{T}{2\pi r_1}\frac{\partial\phi}{\partial a} - \frac{1}{2\pi r_1}\frac{\partial U}{\partial a} \tag{34}$$

The following integral of Maxwell-Mohr is applied in order to derive the angle of twist of the free end of the external crack arm:

$$\phi = \int_0^a M_{1t}\frac{\gamma_f}{r_1}dx + \int_a^l M_{1t}\frac{\gamma_d}{r_2}dx \tag{35}$$

where $x$ is the longitudinal centroidal axis of the shaft (Fig. 2). In (35), $M_{1t}$ is the unit torsion moment applied at the free end of external crack arm. From (35), one derives

$$\phi = \frac{\gamma_f}{r_1}a + \frac{\gamma_d}{r_2}(l - a) \tag{36}$$

The internal crack arm is free of stresses. Therefore, the strain energy cumulated in the shaft is determined by integrating of the strain energy densities in the layers of the external crack arm and the un-cracked shaft portion

$$U = 2\pi a\sum_{i=1}^{i=n2}\int_{r_i}^{r_{i+1}} u_{0a_2 i} r dr + 2\pi(a - l)\sum_{i=1}^{i=n}\int_{r_i}^{r_{i+1}} u_{0i} r dr \tag{37}$$

where the strain energy density in the $i$-th layer of the external crack arm, $u_{0a_2 i}$ is calculated by the following formula [11]:

$$u_{0a_2 i} = \frac{\tau_{fi}^2}{2Q_i} + \frac{\tau_{fi}^{\frac{1+m_i}{m_i}}}{(1+m_i)H_i^{\frac{1}{m_i}}} \tag{38}$$

The strain energy density in the $i$-th layer of the uncracked shaft portion, $u_{0i}$, is written as:

$$u_{0i}=\frac{\tau_{di}^2}{2Q_i}+\frac{\tau_{di}^{\frac{1+m_i}{m_i}}}{\left(1+m_i\right)H_i^{\frac{1}{m_i}}} \tag{39}$$

The final expression for the strain energy release rate is derived by substituting of (36) and (37) in (34)

$$G=\frac{T}{2\pi r_1}\left(\frac{\gamma_f}{r_1}-\frac{\gamma_d}{r_2}\right)- \frac{1}{r_1}\left(\sum_{i=1}^{i=n_2}\int_{r_i}^{r_{i+1}}u_{0a2i}rdr-\sum_{i=1}^{i=n}\int_{r_i}^{r_{i+1}}u_{0i}rdr\right) \tag{40}$$

The integration in (40) should be carried-out by using the MatLab computer program. The strain energy release rates obtained by (40) are exact matches of the strain energy release rates calculated by (1). This fact proofs the correctness of the delamination fracture analysis of multilayered circular shafts developed in the present paper. It should be noted that the strain energy release rate in the clamped shaft is analyzed also by keeping more than three members in the series of Taylor (7). The strain energy release rates obtained are very close to these determined by using the first three members (the difference is less than 2 %).

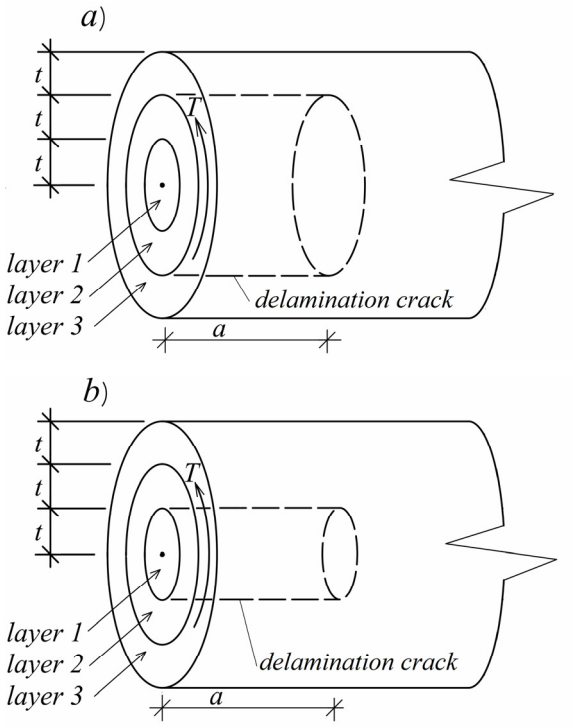


**Figure 3. Fragments of two three-layered circular shaft configurations with a delamination crack located (a) between layers 2 and 3, and (b) between layers 1 and 2**

Parametric investigations are performed in order to appraise the influences of material inhomogeneity, delamination crack location in radial direction of the shaft cross-section and the non-linear mechanical behaviour of the inhomogeneous material on the delamination fracture in the multilayered non-linear elastic clamped circular shaft. For this purpose, calculations of the strain energy release rate are performed by applying the solution (1). The obtained strain energy release rates are presented in non-dimensional form by using the formula $G_N = G/(Q_{01}r_2)$. The material inhomogeneity in radial direction is characterized by $g_{qi}$, $g_{hi}$ and $g_{mi}$. In order to appraise the influence of the delamination crack location on the fracture behaviour, two three-layered shaft configurations are studied. In the first configuration, shown in Figure 3a, a cylindrical delamination crack is located between layers 2 and 3. A shaft configuration with a cylindrical delamination crack between layers 1 and 2 is also studied (Figure 3b).

Both configurations are loaded by a torsion moment, $T$, applied at the free end of external crack arm. The thickness of the layers in both configurations is $t$. It is assumed that $t$ = 0.004 m and $T$ = 20 Nm.

First, the effect of $g_{q1}$ on the delamination fracture behaviour is appraised. The shaft configuration with delamination crack located between layers 2 and 3 is investigated (refer to Figure 3a). The strain energy release rate in non-dimensional form is presented as a function of $g_{q1}$ in Figure 4 assuming that $Q_{02}/Q_{01}$ = 0.7, $Q_{03}/Q_{01}$ = 0.5, $H_{01}/Q_{01}$ = 0.6, $H_{02}/H_{01}$ = 0.5, $H_{03}/H_{01}$ = 0.8, $m_{01} = m_{02} = m_{03}$ = 0.4, $g_{h1} = g_{h2} = g_{h3}$ = 0.6, $g_{m1} = g_{m2} = g_{m3}$ = 0.5. The curves in Figure 4 indicate that the strain energy release rate decreases with increasing of $g_{q1}$ (this behaviour is explained by increase of the shaft stiffness when $g_{q1}$ increases). The strain energy release rate derived assuming linear-elastic mechanical behaviour of the inhomogeneous material is plotted in non-dimensional form against $g_{q1}$ in Figure 4 for comparison with the non-linear solution.

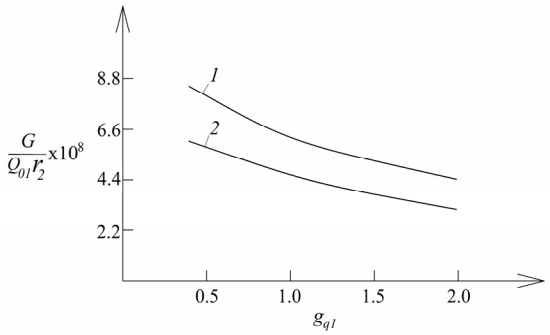


**Figure 4. The strain energy release rate in non-dimensional form presented as a function of $g_{q1}$ at (curve 1) non-linear mechanical behaviour of the inhomogeneous material, and (curve 2) linear-elastic behaviour. The three-layered shaft configuration with a delamination crack located between layers 2 and 3 (refer to Fig. 3a) is analyzed**

The curves in Figure 4 show that the material non-linearity leads to increase of the strain energy release rate. It should be noted that the linear-elastic solution to the strain energy release rate is derived by substituting of $H \rightarrow \infty$ in the non-linear solution (1) because at $H \rightarrow \infty$ the Ramberg-Osgood constitutive law (2) transforms in the Hooke's law assuming that $Q_i$ is the shear modulus of the inhomogeneous material in the $i$-th layer of the shaft.

The influence of $g_{h1}$ on the delamination fracture behaviour is appraised too. For this purpose, the strain energy release rate in non-dimensional form is presented as a function of $g_{h1}$ in Figure 5 at $g_{q1}$ = 0.5

and $g_{m1}$ = 0.5 for both three-layered shaft configurations depicted in Figure 3. It can be observed in Figure 5 that the strain energy release rate decreases with increasing of $g_{h1}$. This finding is attributed to the increase of the stiffness with increasing of $g_{h1}$.

Concerning the effect of the delamination crack location on the delamination fracture behaviour, the curves in Figure 5 indicate that the strain energy release rate is higher when the delamination is between layers 2 and 3.

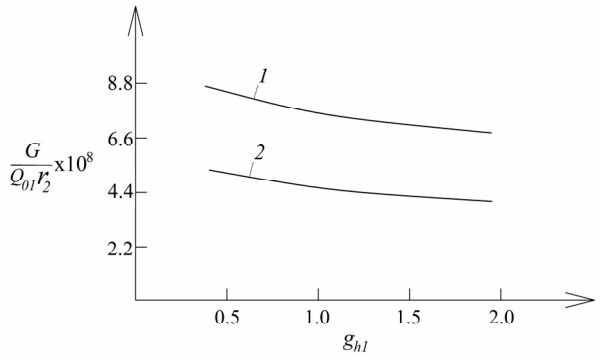


**Figure 5. The strain energy release rate in non-dimensional form presented as a function of $g_{h1}$ for the three-layered shaft configuration with a delamination located (curve 1) between layers 2 and 3, and (curve 2) between layers 1 and 2 (refer to Fig. 3)**

This finding is attributed to the fact that the stiffness of the external crack arm is lower when the delamination is between layers 2 and 3.

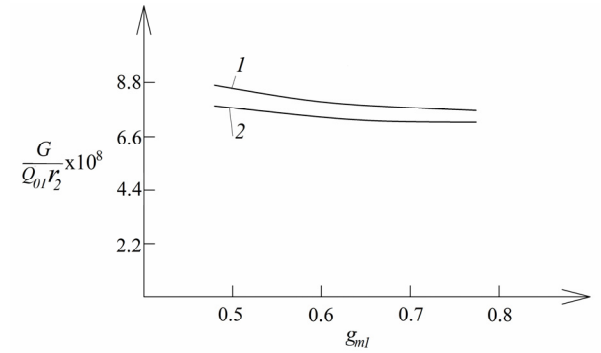


**Figure 6. The strain energy release rate in non-dimensional form presented as a function of $g_{m1}$ at (curve 1) $H_{02}/H_{01}$ = 0.5 and (curve 2) $H_{02}/H_{01}$ = 3.0**

In order to appraise the effect of $g_{m1}$ on the delamination fracture behaviour, the strain energy release rate in non-dimensional form is presented as a function of $g_{m1}$ in Figure 6 at $g_{q1}$ = 0.5 and $g_{h1}$= 0.6 for two $H_{02}/H_{01}$ ratios. The shaft configuration with a delamination crack located between layers 2 and 3 is analyzed. One can observe in Figure 6 that increase of $g_{m1}$ leads to decrease of the strain energy release rate (this is due to the increase of the stiffness). The strain energy release rate decreases also with increasing of $H_{02}/H_{01}$ ratio (Figure 6). This phenomenon is explained by the increase of the stiffness with increasing of $H_{02}/H_{01}$ ratio.

## 4. CONCLUSION

Delamination fracture behaviour of multilayered inhomogeneous non-linear elastic circular shafts loaded in torsion is analyzed in terms of the strain energy release rate. The non-linear elastic behaviour of the material is treated by the Ramberg-Osgood constitutive law assuming that the three material properties involved in the constitutive law vary continuously in radial direction in each layer. A methodology for determination of the strain energy release rate is developed that can be applied for shafts made of layers which have individual thicknesses and material properties. The methodology is used to perform a parametric analysis in order to appraise the influence of material inhomogeneity on the delamination fracture behaviour of the clamped shaft. The analysis reveals that the strain energy release rate decreases with increasing of $g_{q1}$, $g_{h1}$ and $g_{m1}$ (the material properties, $g_{q1}$, $g_{h1}$ and $g_{m1}$, govern the material inhomogeneity in radial direction of layer 1). The influence of delamination crack location in radial direction of the shaft cross-section on the fracture is appraised too. It is found that the strain energy release rate decreases when the stiffness of the external crack arm increases. The effect of material non-linearity on the delamination fracture behaviour is also studied. The analysis shows that the strain energy release rate is higher in multilayered shafts exhibiting non-linear mechanical behaviour of the inhomogeneous material.

The methodology developed in the present paper can be applied in design of multilayered functionally graded shafts with considering of their delamination fracture behaviour. The methodology can be used to check for delamination crack growth. For this purpose, first, the strain energy release rate has to be calculated for a given magnitude of external loading by applying the methodology. The calculated strain energy release rate has to be compared with the delamination fracture toughness in order to check for crack growth. The methodology can be applied also to calculate the strain energy release rate by using experimental data from delamination fracture tests on multilayered inhomogeneous non-linear elastic shafts loaded in torsion.

## REFERENCES


[1] Hutchinson, W. and Suo, Z.: Mixed mode cracking in layered materials, Advances in Applied Mechanic, Vol. 64, pp. 804–810, 1992.

[2] Rizov, V.I.: Delamination fracture in a functionally graded multilayered beam with material nonlinearity, Archive of Applied Mechanics, Vol. 87, pp. 1037-1048, 2017.

[3] Rizov, V.I.: Non-linear elastic delamination of multilayered functionally graded beam, Multidiscipline Modelling in Materials and Structures, Vol. 13, pp. 434-447, 2017.

[4] Rizov, V.I.: Delamination of Multilayered Functionally Graded Beams with Material Nonlinearity, International Journal of Structural Stability and Dynamics, doi.org/10.1142/S0219455418500517, 2017.

[5] Hirai, T., Chen, L.: Recent and prospective development of functionally graded materials in Japan, Mater Sci. Forum, Vol. 308-311, pp. 509-514, 1999.

[6] Bykov, Yu. V., Egorov, S. V., Ermeev, A. G. and Holoptsev, V. V.: Fabrication of metal-ceramic

functionally graded materials by microwave sintering, Inorganic Materials: Applied Research, Vol. 3, DOI: 10.1134/S20751133120300057, 2012.

[7] Moore, J.J.: Self-propagating high-temperature synthesis of functionally graded PVD targets with a ceramic working layer of TiB-TiN or TiSi-Tin, Journal of Materials Synthesis and Processing, Vol. 10, 319. doi:10.1023/A:1023881718671, 2002.

[8] Niranjan, L. and Achchhe, L.: Stochastic dynamic instability response of piezoelectric functionally graded beams supported by elastic foundation, Advances in Aircraft and Spacecraft Science, Vol. 3, pp. 471-502, 2016.

[9] Uslu Uysal, M.: Buckling behaviours of functionally graded polymeric thin-walled hemispherical shells, Steel and Composite Structures, An International Journal, Vol. 21, pp. 849-862, 2016.

[10] Garinis, D., Dinulovic, M., and Rašuo, B.: Dynamic analysis of modified composite helicopter blade, FME Transactions, Vol. 40, No. 2, pp. 63-68, 2012.

[11] Dinulović, M., Rašuo, B., Krstić, B. and Bojanić, A.: 3D random fiber composites as a repair material for damaged honeycomb cores, FME Transactions, Vol. 41, No. 4, pp. 325-332, 2013.

[12] Kastratovic, G., Vidanovic, N., Grbovic, A., Rasuo, B.: Approximate determination of stress intensity factor for multiple surface cracks, *FME Transactions*, Vol. 46, No. 1, pp. 41-47, 2018.

[13] Saghafi, H., Brugo, T., Zucchelli, A., et al.: Comparison the effect of pre-stress and curvature of composite laminate under impact loading. *FME Transactions*: Vol. 44, No. 4, pp. 353-357, 2016.

[14] Rasuo, B.: Experimental techniques for evaluation of fatigue characteristics of laminated constructions from composite materials: full-scale testing of the helicopter rotor blades, Journal of Testing and Evaluation (JTE), Vol. 39, Issue 2, ASTM International, USA, pp. 237-242, 2011.

[15] Rebhi, L., Dinulović, M., Dunjić, M., Grbović, A., Krstić, B.: Calculation of the Effective Shear Modulus of Composite Sandwich Panels, FME Transactions 45 (4), 2017, pp. 537-542.

[16] Purnomo, Soenoko, Suprapto, A. and Irawan, Y.S.: Impact fracture toughness evaluation by essential work of fracture method in high density polyethy–lene filled with zeolite, FME Transactions, Vol. 44, pp. 180-186, 2016.

[17] Zhang, H., Li, X. et al.: Stress intensity factors of double cantilever nanobeams via gradient elasticity theory, Engng. Fract. Mech. Volume 105**,** pp. 58-64, 2013.

[18] Rizov, V. I.: Non-linear fracture in bi-directional graded shafts in torsion, Multidiscipline Modeling in Materials and Structures, Vol. 15(1), pp. 156-169, 2018.

[19] Rizov, V.I.: Elastic-plastic fracture of functionally graded circular shafts in torsion, Advances in Materials Research, Vol. 5, pp. 299-318, 2016.

[20] Rizov, V.I.: Delamination analysis of a layered elastic-plastic beam, International Journal of Structural Integrity, Vol. 8, pp.516-529, 2017.

**NOMENCLATURE**

| | |
|---|---|
| $A$ | crack length |
| $G$ | strain energy release rate |
| $H$ | material property |
| $l$ | length of the delamination crack front |
| $m$ | material property |
| $N$ | number of layers |
| $p$ | coefficient in series of Taylor |
| $Q$ | material property |
| $q$ | coefficient in series of Taylor |
| $r$ | radius of cross-section |
| $s$ | coefficient in series of Taylor |
| $T$ | torsion moment |
| $t$ | thickness of layer |
| $U$ | strain energy |
| $U$ | strain energy density |

***Greek symbols***

| | |
|---|---|
| $\varphi$ | angle of twist |
| $\gamma$ | shear strain |
| $\tau$ | shear stress |
| $\psi$ | material property |

***Subscripts***

| | |
|---|---|
| $\alpha_i$ | subscript of coefficients in series of Taylor |
| $\beta_i$ | subscript of coefficients in series of Taylor |
| $\delta_i$ | subscript of coefficients in series of Taylor |

## ДЕЛАМИНАЦИЈА ВИШЕСЛОЈНЕ ЕЛАСТИЧНЕ ОСОВИНЕ ОПТЕРЕЋЕНЕ ТОРЗИЈОМ

**В. Ризов**

Прслине деламинације код вишеслојних кружних осовина оптерећених торзијом се испитују са аспекта брзине ослобађања деформационе енергије. Полази се од претпоставке да се материјал сваког слоја понаша механички нелинеарно што се анализира применом Рамберг-Озгудовог закона. Сваки слој показује нехомогеност материјала у радијалном правцу. Претпоставља се да три својства материјала, која укључује Рамберг-Озгудов закон, непрекидно варирају у радијалном правцу слојева. Методологија одређивања брзине ослобађања деформационе енергије је развијена тако да се може применити на осовине израђене од произвољног броја конценцитричних слојева спојених адхезијом, при чему сваки слој има одређену дебљину и својства материјала. Места прслина деламинације између слојева су одређена произвољно. Методологија се користи за истраживање деламинације код вишеслојне фиксиране осовине. Деламинација је анализирана и са аспекта енергетске равнотеже у циљу верификације. Извршена је параметарска анализа фиксиране вишеслојне осовине.